Carbohydrate Research, 237 (1992) 249–262
Elsevier Science Publishers B.V., Amsterdam

Structure of the O-antigen of *Escherichia coli* 0119 lipopolysaccharide

A. Nixon Anderson, James C. Richards and Malcolm B. Perry

Institute of Biological Sciences, National Research Council of Canada, Ottawa, Ontario, K1A OR6 (Canada)

(Received April 6th, 1992; accepted June 5th, 1992)

ABSTRACT

The structure of the O-polysaccharide component of the lipopolysaccharide produced by *Escherichia coli* 0119 was determined by the use of methylation analysis, periodate oxidation, 1D and 2D nuclear magnetic resonance spectroscopy, and mass spectrometric methods. The O-polysaccharide was found to be a high molecular weight polymer of a repeating pentasaccharide unit composed of D-mannose, D-galactose, L-rhamnose, 2-acetamido-2-deoxy-D-glucose, and 2-acetamido-2,3-dideoxy-3-formamido-D-rhamnose residues (1:1:1:1:1) and had the structure:

$$[\rightarrow 3)\text{-}\alpha\text{-D-Glc}p\text{NAc-}(1\rightarrow 2)\text{-}\beta\text{-D-Man}p\text{-}(1\rightarrow 3)\text{-}\alpha\text{-D-Gal}p\text{-}(1\rightarrow 4)\text{-}\alpha\text{-L-Rha}p\text{-}(1\rightarrow]_n$$

$$\begin{array}{c} 3 \\ \uparrow \\ 1 \\ \beta\text{-D-Rha}p2\text{NAc3NFo} \end{array}$$

INTRODUCTION

Escherichia coli 0119 is an enteropathogenic (EPEC) serotype that has been identified as one of the major causative organisms involved in severe infantile diarrhoea[1,2]. During the course of the disease, some bacteria adhere to and colonize the luminal wall of the gastrointestinal tract thereby causing local histological damage to the epithelium which results in a protraction of the disease state[3]. The mechanism involved in the adhesion of the bacteria is unclear, however there is in vitro evidence of the involvement of plasmid-mediated factors in the process[4]. Smooth clinical isolates of *E. coli* 0119 have shown a strain-specific difference in their ability to adhere to HEp-2 cells[5]. SDS-PAGE analysis of the lipopolysaccharides (LPSs) isolated from these isolates indicated structural differences in the LPS core regions which correlate with the adhesive property of the

Correspondence to: Dr. M.B. Perry, Institute of Biological Sciences, National Research Council of Canada, Ottawa, ON, K1A OR6, Canada.

bacterial strain[6]. The present investigation was undertaken to determine the chemical nature of the LPS O-chains isolated from an adhesive strain of *E. coli* 0119 (JCP88, NRCC 4326) and from a nonadhesive strain (19392, NRCC 4325). It was found that the LPS O-chains produced by the two strains were identical in their fine structures and that they determine the 0119 serospecificity.

RESULTS AND DISCUSSION

0119 LPS.—LPS was isolated in ~6% yield from *E. coli* 0119 (JCP88, NRCC 4326) cells using the hot aqueous phenol method[7,8]. Partial hydrolysis of the LPS with hot dilute acetic acid gave a lipid A (12% yield), as an insoluble precipitate, and a water-soluble carbohydrate fraction. This latter material was separated by gel filtration on a Sephadex G-50 column to give three fractions, which were identified by chemical analyses as being the following: (*1*) O-polysaccharide (27% yield, $[\alpha]_D$ +86.24° (*c* 13.5, H_2O), K_{av} 0.15), (*2*) core oligosaccharide (24%, $[\alpha]_D$ +97.40° (*c* 21.4, H_2O), K_{av} 0.72), and (*3*) a fraction containing 3-deoxy-D-*manno*-2-octulosonic acid (D-Kdo) and phosphate (17%, K_{av} 1.00).

LPS from *E. coli* 0119 (19392, NRCC 4325) cells (~4% yield) was also isolated and, upon partial hydrolysis as described above, gave a lipid A (18% yield), O-polysaccharide (23%, $[\alpha]_D$ +84.85° (*c* 11.5, H_2O), K_{av} 0.15), core oligosaccharide (19%, $[\alpha]_D$ +120.20° (*c* 9.8, H_2O), K_{av} 0.65) and a D-Kdo–phosphate fraction (15%, K_{av} 1.00) after chromatographic separation.

Analysis of the O-polysaccharide.—Chemical analyses and NMR data for the O-polysaccharide from NRCC 4325 and NRCC 4326 showed that the two O-chains had the same repeating unit structure. Accordingly, the results presented and discussed below have been confined to those obtained for the latter strain.

Microanalysis of the 0119 polysaccharide gave: C, 40.30; H, 5.70; and N, 3.18, with a zero ash value. Glycose analysis (Table I, column 1) after hydrofluoric acid–trifluoroacetic acid (HF–TFA) hydrolysis indicated the presence of L-Rha, D-Man, D-Gal and D-GlcN in a molar ratio of 0.9 : 0.2 : 1.0 : 1.7. Stronger hydrolytic conditions using concd HCl resulted in the detection of a greater molar ratio of D-Man but with a concomitant reduction in the ratios of L-Rha and D-GlcN (Table I, column 2). The absolute configuration of the above sugar residues were determined by GLC analysis of their peracetylated or trimethylsilylated (*R*)-2-butyl glycoside derivatives[9,10] (Table I).

Methylation analysis of the 0119 polysaccharide (Table II, column 1) indicated the presence of residues of an *O*-4 linked L-Rha*p*, an *O*-3 linked D-Gal*p*, an *O*-3 linked D-Glc*p*N, and a branch-point *O*-2,3-disubstituted D-Man*p*. The presence of a terminal, nonreducing sugar residue, expected from the detection of the branch-point D-Man*p* derivative, was not detected in the methylation analysis.

An examination of the ^{13}C NMR spectrum of the O-polysaccharide (Table III) showed the following characteristic signals: five major signals in the pyranose

TABLE I

Sugar analyses of *E. coli* 0119 polysaccharide and derived products

Sugar [a] (as alditol acetate)	Molar ratio [b,c]					
	1	2	3	4	5	6
4-Deoxy-L-erythritol					1.68	0.67
L-Rha	0.88	0.19	0.96	0.83		
2,5-Anhydro-D-mannitol			1.55			
D-Man	0.23	0.56	0.82	0.63	0.19	0.25
D-Gal	1.00	1.00	1.00	1.00	1.00	1.00
D-GlcNAc	1.73	1.26		0.84	0.92	

[a] For assignment of the absolute configurations, see Experimental. [b] Determined on a DB-17 capillary column, see Experimental for details. [c] 1, 0119 polysaccharide (HF–TFA hydrolysis); 2, 0119 polysaccharide (concd HCl hydrolysis); 3, deacylated–deaminated product; 4, partially deacylated–deaminated product; 5, O*1*; and 6, O*2*.

anomeric carbon region (97–102 ppm), three signals for deoxyamino-substituted carbon atoms (52–54 ppm), two 6-deoxyhexose methyl carbon resonances (~ 17.7 ppm), signals for two *N*-acetyl substituents (~ 22.7 ppm (CH_3CONH) and 174–176 ppm (CH_3CONH)), and for an *N*-formyl substituent (HCONH) at 165.16 and 168.23 ppm (9:1 rotameric effect). A coupled ^{13}C NMR spectrum indicated the presence of three α- and two β-anomeric linkages[11], which were assigned by comparison with the data in Table IV. Consistent with the ^{13}C NMR spectrum, the ^1H NMR spectrum of the O-polysaccharide (Table III) showed five anomeric proton signals (4.8–5.3 ppm), two overlapping methyl doublets for 6-deoxyglycose residues (1.33 ppm), two overlapping *N*-acetyl methyl resonances (2.02 ppm), and a singlet (8.05 ppm) characteristic of an *N*-formyl substituent.

TABLE II

Methylation analyses of *E. coli* 0119 polysaccharide and derived products

Methylated sugar [a] (as alditol acetate)	t_R [b]	Molar ratio [c,d]				
		1	2	3	4	5
1,4,6-Anhydromannitol	0.55		0.23			
2,3,4-Rha	0.68			0.18		
2,3-Rha	0.89	1.75	0.59	0.97		
2,3,4,6-Man	1.00		0.93	0.37		
3,4,6-Man	1.31			0.70		
2,4,6-Man	1.42					0.53
2,4,6-Gal	1.46	1.00	1.00	1.00	1.00	1.00
4,6-Man	1.73	0.50			0.64	
3,4,6-GlcNAc	2.65			0.21	0.79	
4,6-GlcNAc	3.75	0.37		0.32		

[a] 2,3,4-Rha = 1,5-di-*O*-acetyl-2,3,4-tri-*O*-methylrhamnitol, etc.; all substitution patterns were confirmed by GLC–MS. [b] Retention time relative to that of 1,5-di-*O*-acetyl-2,3,4,6-tetra-*O*-methylglucitol. [c] Determined on a DB-17 capillary column; see Experimental for details. [d] 1, 0.119 polysaccharide; 2, deacylated–deaminated product; 3, partially deacylated–deaminated product; 4, O*1*; and 5, O*2*.

TABLE III

NMR data (500 MHz) for *E. coli* 0119 O-chain polysaccharide

→ 3)-α-D-Glc*p*NAc-(1 → 2)-β-D-Man*p*-(1 → 3)-α-D-Gal*p*-(1 → 2)-α-L-Rha*p*-(1 →
3
↑
1
β-D-Rha*p*2NAc3NFo

0119 O-Chain Polysaccharide

^{1}H NMR data [a]		^{13}C NMR data [b]	
δ	Assignment [c]	δ ($J_{C,H}$) [d]	Assignment
8.05	*H*CONH (Rha2NAc3NFo)	175.54	CH_3CO (Rha2NAc3NFo)
5.31	H-1 (α-D-GlcNAc)	174.15	CH_3CO (GlcNAc)
5.07	H-1 (α-D-Gal)	168.23	HCONH (Rha2NAc3NFo)
4.98	H-1 (α-D-Rha2NAc3NFo) [e]	165.16	HCONH (Rha2NAc3NFo)
4.94	H-1 (β-D-Man) [e]	102.16(159)	C-1 (β-D-Rha2NAcNFo)
4.86	H-1 (α-L-Rha)	101.85(169)	C-1 (α-L-Rha)
4.53	H-2 (Rha2NAc3NFo)	101.64(162)	C-1 (β-D-Man)
4.45	H-2 (Man)	100.55(170)	C-1 (α-D-Gal)
3.31	H-4 (Rha2NAc3NFo)	97.50(177)	C-1 (α-D-GlcNAc)
2.02	CH_3CO (GlcNac)[f]	53.94	C-2 (GlcNAc)
	(Rha2NAc3NFo) [f]	53.04	C-3 (Rha2NAc3NFo)
1.33	CH_3 (Rha) [g]	52.15	C-2 (Rha2NAc3NFo)
	(Rha2NAc3NFo) [g]	22.87	CH_3CO (Rha2NAc3NFo)
		22.56	CH_3CO (GlcNAc)
		17.79	CH_3 (Rha2NAc3NFo)
		17.64	CH_3 (Rha)

[a,b] Chemical shifts are measured in ppm with reference to internal acetone, δ 2.225 for ^{1}H NMR and 31.07 ppm for ^{13}C NMR. [c] Assignments are made with reference to those in Table IV. [d] Coupling constants are measured in Hz. [e] These assignments may be interchanged. [f,g] Unresolved signals.

The above preliminary data indicate that the 0119 LPS O-chain is composed of a regular repeating pentasaccharide unit composed of D-Man*p*, D-Gal*p*, L-Rha*p*, D-Glc*p*N, and an unidentified trideoxydiaminoglycose residue. Attempts to isolate and characterize the trideoxydiaminoglycose residue using established procedures[12] involving hydrolysis, methanolysis, hydrofluorinolysis, and mercaptolysis were unsuccessful. The residue was, however, subsequently identified by detailed NMR spectroscopy and mass spectrometry (MS). In order to further characterize the O-chain, the polymer was subjected to deamination and sequential periodate oxidation degradations.

Deamination.—Nitrous acid deamination[13] of a completely *N*-deacylated sample of O-chain (thiophenol–NaOH method[14]), evidenced from ^{1}H NMR spectroscopy, followed by reduction ($NaBH_4$) gave a product composed of L-Rha, D-Man, D-Gal, and 2,5-anhydro-D-mannitol (1.0 : 0.8 : 1.0 : 1.6) (Table I, column 3). Methylation analysis of this product (Table II, column 2) indicated, *inter alia*, the presence of 3-*O*-acetyl-2,5-anhydro-1,4,6-tri-*O*-methylmannitol and 2,3,4,6-tetra-*O*-methylmannitol, indicating that the 3-*O* substituted D-Glc*N*p is linked to either the *O*-2 or *O*-3 position of the D-Man*p* residue in the intact O-chain. The

TABLE IV

NMR data (500 MHz) for oligosaccharides O*1* and O*2*

Unit (**a**) Unit (**b**) Unit (**c**) Unit (**d**)

O*1*: α-D-Glc*p*NAc-(1 → 2)-β-D-Man*p*-(1 → 3)-α-D-Gal*p*-(1 → 2)-L-4-Deoxy-Eryol

3
↑
1

β-D-Rha*p*2NAc3NFo

Unit (**e**)

O*2*: β-D-Rha*p*2NAc3NFo-(1 → 3)-β-D-Man*p*-(1 → 3)-α-D-Gal*p*-(1 → 2)-L-4-Deoxy-Eryol

	Unit (**e**)	Unit (**b**)	Unit (**c**)	Unit (**d**)	
^{1}H NMR [a]	O*1*	O*2*	^{13}C NMR [b]	O*1*	O*2*
Unit **a**					
H-1($J_{1,2}$)	5.31(3.7)		C-1($J_{C,H}$)	97.29(175)	
H-2($J_{2,3}$)	3.91(9.6)		C-2	54.30	
H-3($J_{3,4}$)	3.82(10.0)		C-3	72.01	
H-4($J_{4,5}$)	3.48(9.4)		C-4	70.46	
H-5($J_{5,6}$)	4.28(6.5)		C-5	71.74	
($J_{5,6'}$)	(2.2)				
H-6($J_{6,6'}$)	3.79(12.0)		C-6	61.22	
H-6′	3.79				
CH_3CO	1.99		CH_3CO	22.72 [c]	
			CH_3CO	174.25	
Unit **b**					
H-1($J_{1,2}$)	4.92(1.3)	4.87(< 1)	C-1($J_{C,H}$)	102.44(163)	101.91
H-2($J_{2,3}$)	4.44(2.4)	4.33(3.1)	C-2	74.29	71.02
H-3($J_{3,4}$)	3.83(9.9)	3.78(9.4)	C-3	83.34	82.74
H-4($J_{4,5}$)	3.76(8.2)	3.65(9.7)	C-4	66.98	66.37
H-5($J_{5,6}$)	3.41(8.4)	3.38(5.8)	C-5	77.33	76.74
($J_{5,6'}$)	(3.5)	(2.2)			
H-6($J_{6,6'}$)	3.78(9.5)	3.69(12.4)	C-6	61.38	61.65
H-6′	3.92	3.88			
Unit (**c**)					
H-1($J_{1,2}$)	5.12(4.2)	5.15(4.0)	C-1($J_{C,H}$)	99.29(169)	99.29
H-2($J_{2,3}$)	3.90(9.6)	3.96(10.5)	C-2	68.80	68.60
H-3($J_{3,4}$)	4.02(2.9)	4.07(2.9)	C-3	79.84	79.11
H-4($J_{4,5}$)	4.17(< 1)	4.22(< 1)	C-4	69.74	70.14
H-5($J_{5,6}$)	4.12(2.0)	4.16(8.8)	C-5	72.01	71.50
($J_{5,6'}$)	(10.0)	(8.8)			
H-6($J_{6,6'}$)	3.69(12.0)	3.72(12.0)	C-6	61.75	61.81
H-6′	3.71	3.72			
Unit (**d**)					
H-1($J_{1,2}$)	3.76(6.0)	3.77(6.9)	C-1	61.58	61.65
H-1′($J_{1',2}$)	3.76(2.7)	3.77(2.7)			
($J_{1,1'}$)	(11.3)	(11.5)			
H-2($J_{2,3}$)	3.64(4.4)	3.65(4.3)	C-2	83.11	83.15
H-3($J_{3,4}$)	4.04(6.6)	4.05(6.5)	C-3	67.44	67.46
H-4[CH_3]	1.23	1.23	C-4	18.32	18.33

TABLE IV (Continued)

^{1}H NMR [a]	O*1*	O*2*	^{13}C NMR [b]	O*1*	O*2*
Unit (e)					
H-1($J_{1,2}$)	4.94($\approx$1)	5.05(1.6)	C-1($J_{C,H}$)	101.78(160)	101.18
H-2($J_{2,3}$)	4.50(3.8)	4.57(4.0)	C-2	52.11	52.36
H-3($J_{3,4}$)	4.05(10.5)	4.09(10.3)	C-3	53.03	52.91
H-4($J_{4,5}$)	3.28(9.4)	3.33(9.5)	C-4	70.59	70.67
H-5($J_{5,6}$)	3.50(6.2)	3.55(6.1)	C-5	74.67	74.66
H-6[CH_3]	1.32	1.33	C-6	17.79	17.86
*H*CONH	8.03	8.06	HCONH	165.14	165.21
				168.20	168.26
CH_3CO	2.04	2.09	CH_3CO	22.72 [c]	22.93
			CH_3CO	175.70	176.36

[a,b] Chemical shifts are measured in ppm with reference to internal acetone, δ 2.225 for ^{1}H NMR and 31.07 ppm for ^{13}C NMR. Measured coupling constants were refined by spectral simulation and are given in Hz. [c] Unresolved signals.

presence of the tetra-*O*-methylmannitol derivative indicates that the two residues linked to the original D-Man*p* residues were both susceptible to the deamination procedure; however, the second glycose residue was not identified.

A partially *N*-deacylated sample of O-chain (NaOH hydrolysis), which showed essentially only a single *N*-acetyl methyl resonance in its ^{1}H NMR spectrum, on nitrous acid deamination and reduction ($NaBH_4$) gave a product which on hydrolysis afforded D-Man, L-Rha, D-Gal, and D-GlcN (0.6 : 1.0 : 1.0 : 0.8) (Table I, column 4) but no 2,5-anhydro-D-mannitol, indicating that in the partially *N*-deacylated O-chain the D-GlcN residues were *N*-acetylated, and thus the other *N*-acetyl and the *N*-formyl substituent must be located on the unidentified glycose residue in the native O-chain. Methylation analysis of the product (Table II, column 3) gave 1,2,5-tri-*O*-acetyl-3,4,6-tri-*O*-methylmannitol, indicating that the unidentified aminoglycose was linked to the *O*-3 position of the D-Man*p* branch point in the native O-chain. The absence of 2,4,6-tri-*O*-methylmannose in the hydrolysate of the methylated product substantiates the contention that the D-Man*p* residues in the O-chain are substituted at *O*-2 by D-Glc*p*NAc residues.

Periodate oxidation.—Periodate oxidation[15] of the 0119 polysaccharide, followed by reduction, produced a high molecular weight polymer, which was purified by gel filtration on a Sephadex G-50 column. Smith-type hydrolysis of the polymer gave the pentasaccharide alditol, O*1* (Table IV), indicating that the residue which was susceptible to oxidation by periodate formed part of the backbone of the polysaccharide. Composition and methylation analyses of O*1* (Table I, column 5; Table II, column 4) showed that only the *O*-4 linked L-Rha*p* residue of the O-polysaccharide had been cleaved and that this residue was attached to the *O*-3 linked D-Glc*p*NAc residue, which occupies a terminal, nonreducing position in O*1*. The analysis failed to detect products of the unidentified diaminoglycose component.

The above results indicated that O*1* would be further susceptible to periodate oxidation at its nonreducing D-Glc*p*NAc endgroup. O*1* was thus subjected to a

second periodate oxidation and Smith type hydrolysis which gave the tetrasaccharide alditol, O2 (Table IV). Composition and methylation analyses of O2 (Table I, column 6; Table II, column 5) showed that the D-Glc*p*NAc residue had been eliminated. The methylation analysis indicated that this D-Glc*p*NAc residue had been linked to the *O*-2 position of the D-Man*p* residue, confirming the conclusions drawn from the deamination studies.

NMR analysis of O1 and O2.—NMR analysis of O*1* and O2 using 2D ^{1}H and ^{13}C spectroscopy (CHORTLE[16] and COSY[17] experiments) gave the data collected in Table IV. This data is consistent with the following structures for the oligosaccharides:

Unit (**a**) Unit (**b**) Unit (**c**) Unit (**d**)

O*1*: α-D-Glc*p*NAc-(1 → 2)-β-D-Man*p*-(1 → 3)-α-D-Gal*p*-(1 → 2)-L-4-Deoxy-Eryol

3
↑
1

β-D-Rha*p*2NAc3NFo

Unit (**e**)

O*2*: β-D-Rha*p*2NAc3NFo-(1 → 3)-β-D-Man*p*-(1 → 3)-α-D-Gal*p*-(1 → 2)-L-4-Deoxy-Eryol

Unit (**e**) Unit (**b**) Unit (**c**) Unit (**d**)

From analysis of the COSY and relayed COSY experiments, the proton resonances associated with all of the glycosyl residues were identified (Fig. 1). The chemical-shift data, together with the magnitude of the coupling constants, confirmed that each residue has a pyranose ring form and distinguished those residues that have *gluco* (unit **a**), *galacto* (unit **c**) and *manno* (units **b** and **e**) configurations[18] (Table IV). From the $J_{1,2}$ coupling constants[11], units **a** and **c** were both identified as having the α-anomeric configuration. Correspondingly, the $^{1}J_{C,H}$ coupling constants confirmed these assignments and also established that units **b** and **e** have the β-anomeric configuration. The latter assignments were confirmed from subsequent NOE experiments. Units **a** and **e** were identified as the D-Glc*p*NAc and trideoxydiaminomannose residues, respectively, from the ^{13}C NMR chemical-shift values which were diagnostic of aminodeoxyglycoses.

The sequence of O*1* was unequivocally determined by NOE experiments (Table V). Measurements were determined in the difference mode at 500 MHz, for which negative NOE values were observed. Transglycosidic NOEs were observed between the anomeric and aglyconic protons of contiguous residues, establishing the sequence of the oligosaccharide. The anomeric proton signals from units **b** and **e** were partially overlapping; however, a distinction could be made by selectivity irradiating the high-field portion of the signal. Intraresidue NOEs were observed between H-1 and H-2 of each of the residues and, in addition, units **b** and **e** showed NOEs to their respective H-3 and H-5 protons, clearly establishing their β-anomeric configuration.

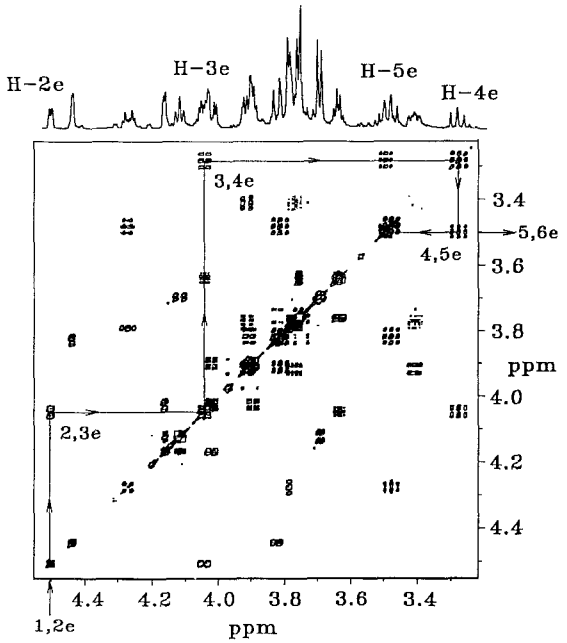

Fig. 1. COSY contour plot for the non-anomeric ring proton region (3.2–4.6 ppm) of oligosaccharide O*1*. The 1D ^{1}H NMR spectrum is shown above, and the connectivity pathway and proton assignments for the 2-acetamido-2,3-dideoxy-3-formamido-β-D-rhamnopyranosyl residue (unit **e**) are indicated.

TABLE V

Nuclear Overhauser enhancement (NOE) observations for O*1* and O*2*

Oligosaccharide [a]	Irradiated proton [b]	Observed proton		Partial sequence
		Intraresidue	Interresidue	
O*1* [c]	H-1**a**	H-2**a**	H-2**b**	**a**(1 → 2)**b**
	H-1**b**	H-2**b**	H-3**c**	**b**(1 → 3)**c**
		H-3**b**		
		H-5**b**		
	H-1**c**	H-2**c**	H-2**d**	**c**(1 → 2)**d**
	H-1**e**	H-2**e**	H-3**b**	**e**(1 → 3)**b**
		H-3**e**		
		H-5**e**		
O*2*	H-1**e**	H-2**e**	H-2**b**	
		H-3**e**	H-3**b**	**e**(1 → 3)**b**
		H-5**e**		
	H-2**e**	H-1**e**		
		H-3**e**		

[a] See text for detailed structures. [b] H-1 **a** denotes the H-1 proton of unit **a** of the oligosaccharide, as defined in the text. [c] Anomeric signals for units **b** and **e** were partially overlapping; however, a distinction could be made by selective irradiation of the high-field portion of the overlapping signal.

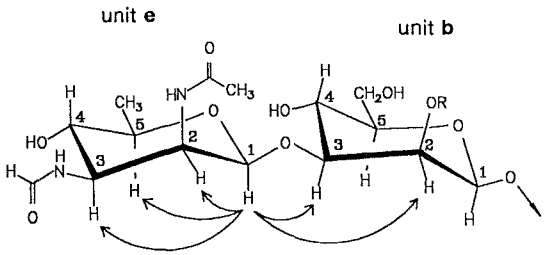

Fig. 2. Structure of the β-D-Rha*p*2NAc3NFo-(1 → 3)-D-Man*p*-(1 → disaccharide moiety: oligosaccharide *O1*; (R = α-D-Glc*p*NAc-(1 →; oligosaccharide *O2* (R = H). Through-space connectivities are identified by the $^1H-^1H$ NOE measurements indicated.

For *O2*, positive NOEs were observed at 200 MHz. Irradiation of H-1 of the trideoxydiaminomannose residue (unit **e**) showed enhancements at both H-2 and H-3 of the β-D-Man*p* residue (unit **b**), confirming the linkage at *O*-3 of this latter residue. The occurrence of an interresidue NOE between H-1 of unit **e** and H-2 of unit **b** can only occur if both glycopyranosyl units possess the same absolute configuration, see (Fig. 2). Since the absolute configuration of the β-Man*p* residue was established as D, then it follows that the trideoxydiaminomannose residue has a D-configuration[19].

The acyl substitution pattern of the trideoxydiaminoglycose residue was determined by selective INEPT[20] experiments, which identify three-bond proton–carbon connectivities. For *O2*, a connectivity was observed between H-2 of unit **e** and the carbonyl carbon of the *N*-acetyl substituent, establishing *N*-acetylation at C-2. In addition, connectivities were observed between H-3 of the same unit and the carbonyl carbon of both the *E*- and *Z*-rotamers of the *N*-formyl substituent, showing the formamido substituent to be at C-3. The accumulated data given above establishes the trideoxydiaminomannose residue to be 2-acetamido-2,3-dideoxy-3-formamido-β-D-rhamnopyranose.

Mass spectrometric analysis of O1 and O2.–Positive FABMS of *O1* showed a molecular ion peak at *m/z* 848 [M + H] and fragment peaks arising via pathways A–C, as defined by Dell[21] (see Table VI). Peaks at *m/z* 742 [M − Ald] and 580 [M − HexAld] confirmed the sequence of *O1*, while that at *m/z* 204 reaffirmed the presence of an *N*-acetylated, terminal D-Glc*p*N residue. The fragment at *m/z* 215 was interpreted as being from an acetamido-formamido-trideoxyhexose residue. The presence of a fragment of mass *m/z* 170 [215 − 45] and the absence of a significant peak at *m/z* 156 [215 − 59] indicate that the formamido function was present at C-3 of the diamino residue[10]. Pathway B and C fragments from the [M + H] molecular ion species were also observed and helped corroborate the structure given for *O1*. Fragments of *m/z* 377 and 366 were interpreted as being derived from the β cleavage (pathway B) of the *m/z* 580 fragment, while those at *m/z* 539 and 528 were similarly derived from the *m/z* 742 fragment. The intensity of the *m/z* 366 fragment may have been augmented by fragments from the matrix.

TABLE VI

Mass spectral data for O*1*, O*2*, and derived products

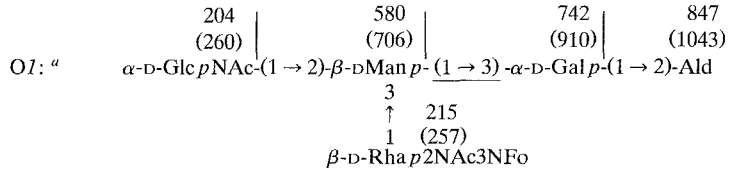

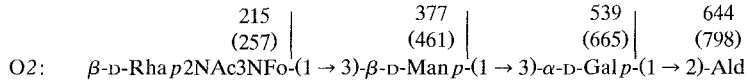

Oligosaccharide	FABMS mode [b]	Pathway [c,d]			Other fragment peaks
		A	B	C	
O*1* [M] = 847	+	742(3) 580(2) 216(26) 215(100) 205(26) 204(100)	645(11) 634(9) 431(2) 269(6) 268(2)	760(3) 598(3) 233(10) 232(3) 222(7) 221(2)	848(72) 847(6) 539(3) 528(2) 377(10) 366(24) 170(68)
O*1* [M + H] ion *m/z* 848	+ CID-B/E	742(3) 580(2) 215(4) 204(4)	645(4) 634(2)		848(100) 539(3) 528(1) 377(2) 366(1) 170(1)
O*1* [M] = 847	−		643(28) 632(23) 429(13) 267(17) 105(24)	758(8) 596(10) 231(25) 220(16)	847(28) 846(60) 671(7)
O*1* [M-H] ion *m/z* 846	− CID-B/E		643(2) 632(2) 267(1)	231(1) 220(1)	846(100)
Permethylated O*1* [M] = 1043	+	910(5) 706(9) 261(94) 260(100) 258(18) 257(51)		274(48)	1066(100) 1044(41) 1012(14) 998(32) 984(12) 966(5) 242(19) 228(100) 198(56) 196(15) 187(17) 184(12) 166(14)

TABLE VI (Continued)

Oligosaccharide	FABMS mode [b]	Pathway [c,d]			Other fragment peaks
		A	B	C	
O2	+	539(6)		106(10)	645(57)
[M] = 644		377(15)			170(39)
		215(100)			156(7)
Permethylated		655(1)			198(14)
O2		461(33)			184(2)
[M] = 798		257(100)			

[a] Where "Ald" refers to a 4-deoxy-L-erythritol residue and "Rha*p*2NAc3NFo" to a 2-acetamido-2,3-dideoxy-3-formamido-D-rhamnose residue. Relevant molecular masses for components of O*1* and O*2*, together with those of the permethylated derivatives in parentheses, have been shown. [b] For details, see Experimental. [c] Pathways as defined by Dell [21]. [d] *M/z* ratio given with relative percentage abundance in parentheses.

A collision-induced dissociation-B/E (CID-B/E) linked scan spectrum of the positive-ion FAB molecular ion species at *m/z* 848 confirmed the primary fragmentation of O*1* and also showed some secondary fragmentation. Data for the negative-ion FABMS of O*1* and CID-B/E linked scan of the molecular ion species at *m/z* 846 [M − H] (Table VI) support the O*1* structure as given.

Positive-ion FABMS analysis of permethylated O*1* helped to conclusively sequence the oligosaccharide alditol. As can be seen from Table VI, the majority of significant fragments from the permethylated derivative resulted either from A_1-type cleavage (pathway A), with or without subsequent fragmentation, or from cleavage of the terminal alditol residue. Of the former, the most significant peak was that at *m/z* 706, which confirmed the position of the branch-point within O*1*. The ions at *m/z* 198 and 166 were interpreted as resulting from the sequential loss of the formamido group at C-3 (as $NHCH_3CHO$) and the methoxy group at C-4 (as CH_3OH) from the A_1-type fragment ion of the diamino residue (*m/z* 257). The analogous series (*m/z* 260, 228, and 196) was seen for the Glc*p*NAc residue. Less significant peaks at *m/z* 184 and 187 were from the elimination of the acetamido substituent at C-2 (as $NHCH_3Ac$) from each of the above A_1-type ions, respectively. The 4-deoxyalditol residue at the reducing end of permethylated O*1* cleaved to give fragments at *m/z* 1012, 998, 984, and 966.

Fragmentation by positive-ion FABMS of O*2* gave a molecular ion species at *m/z* 645 [M + H] and pathway A fragments at *m/z* 539, 377, and 215 which resulted from sequential cleavages from the oligosaccharide alditol. A large peak at *m/z* 170 and a small peak at *m/z* 156 were interpreted as being from the loss of the formamido and the acetamido group, respectively, from the fragment at *m/z* 215 and thus gave supporting evidence for the presence of a formamido group at C-3 of the diamino glycose[21]. Direct-probe EIMS of permethylated O*2* gave, *inter alia*, a molecular ion peak at *m/z* 798 and A_1-type fragments at *m/z* 665, 461, and 257. Once again, the ion at *m/z* 257 fragmented to give either a

large peak at m/z 198 [257 – $NHCH_3CHO$] or a significantly smaller peak at m/z 184 [257 – $NHCH_3Ac$], see Table VI.

CONCLUSIONS

From the accumulated evidence, the structure of the *E. coli* 0119 O-antigen is concluded to be a high molecular weight polymer of repeating branched pentasaccharide units having the structure:

$$[\rightarrow 3)\text{-}\alpha\text{-D-Glc}p\text{NAc-}(1\rightarrow 2)\text{-}\beta\text{-D-Man}p\text{-}(1\rightarrow 3)\text{-}\alpha\text{-D-Gal}p\text{-}(1\rightarrow 4)\text{-}\alpha\text{-L-Rha}p\text{-}(1\rightarrow]_n$$
$$\begin{array}{c} 3 \\ \uparrow \\ 1 \end{array}$$
$$\beta\text{-D-Rha}p2\text{NAc3NFo}$$

The 2-acetamido-2,3-dideoxy-3-formamido-β-D-rhamnose residue has not previously been reported. However, an analogous 2,3-diaminomannuronic acid has been found in *Pseudomonas aeruginosa* O:3a,b lipopolysaccharide[23]. Since it is possible that the trideoxydiaminomannose residue is a major epitopic feature of the *E. coli* 0119 O-antigen, the synthesis of the glycose has been undertaken and its serological relevance is being explored.

EXPERIMENTAL

Analytical methods.—Unless otherwise specified, analytical GLC–MS was done with a Hewlett Packard 5985 GLC–MS system, operating in the EI mode and using an OV-17 fused silica capillary column (Quadrex Corp.). The following temperature programs were employed: A, 180°C for 2 min, then 4°C/min to 240°C (for alditol acetates); B, 200°C for 2 min, then 1°C/min to 240°C (for partially methylated alditol acetates); C, 180°C for 2 min, then 2°C/min to 240°C (for peracetylated (*R*)-2-butyl glycosides); and D, 140°C for 2 min, then 4°C/min to 200°C (for per-*O*-trimethylsilylated (*R*)-2-butyl glycosides).

FABMS analyses were carried out using a JEOL AX505H double-focusing mass spectrometer operating at an accelerating voltage of 3 kV and a mass resolution of 1500. Glycerol–thioglycerol (1:3) or *m*-nitrobenzyl alcohol were used as the supporting matrix for underivatized or permethylated oligosaccharides, respectively. The matrix was applied to the probe tip and was mixed with a solution (1 μL) of the sample in water or CH_2Cl_2. An Xe atom beam of 6 kV was used to sputter and ionize the sample, and spectra were calibrated with Ultramark 1621. Collision induced dissociation FABMS–MS experiments on [M + H] ions were performed using He as the collision gas. Linked scans at constant B/E were generated by the JEOL complement data system.

Samples ($\sim$ 1 mg) were hydrolyzed using 4 M TFA (1 mL, 125°C, 1 h) and the constituent glycoses were determined by GLC–MS of their peracetylated alditol acetate derivatives[23]. Acetolysis, hydrolysis (concd HCl), methanolysis, hydrofluori-

nolysis, and mercaptolysis were performed as described[12]. Methylation of samples (~ 3 mg) was carried out by the Hakomori method[24] as modified by Sandford and Conrad[25], using potassium methylsulfinylmethylide.

NMR spectroscopy.—Unless otherwise specified, spectra were obtained from D_2O solutions of samples at 27°C using a Bruker AM 500 spectrometer equipped with an Aspect 3000 computer using standard Bruker software. ^1H NMR spectra, recorded at 500 MHz, were obtained using a 90° pulse, a spectral width of 2.4 kHz. Chemical shifts are expressed relative to internal acetone (2.225 ppm). Broad-band ^{13}C NMR spectra were obtained at 125 MHz using a 90° pulse, a spectral width of 31 kHz, and WALTZ decoupling with acetone as internal reference (31.07 ppm). $^1J_{C,H}$ values were determined using gated decoupling.

NOE difference spectra[26] were obtained at 500 MHz or at 200 MHz using a Bruker AM 200 spectrometer by sequential saturation of each line of a multiple resonance for a total irradiation time of 400 ms.

Two-dimensional homonuclear chemical shift correlation experiments (COSY and relayed COSY) were carried out as previously described[27] using spectral widths of 2400 or 900 Hz. Heteronuclear ^{13}C–^1H one- and three-bond chemical shift correlations were carried out using the CHORTLE[16] and selective INEPT[20] pulse sequences, respectively.

Preparation and properties of 0119 polysaccharide.—E. coli 0119 (JCP88, NRCC 4326 and 19392, NRCC 4325) were grown (yield 10 g wet wt/L), and the LPS was isolated as previously described[6]. Partial hydrolysis of LPS (2.5 g) with acetic acid (1.5%, 200 mL, 100°C, 2 h) gave an insoluble lipid A fraction (0.29 g) and a carbohydrate fraction (1.83 g), which was fractionated by Sephadex G-50 gel-filtration chromatography using a 0.05 M pyridinium acetate buffer at pH 4.6. Collected fractions (10 mL) were analyzed for neutral glycose by the phenol–H_2SO_4 method[24], aminodeoxyglycose by a modified the Elson–Morgan method[25], and for Kdo[26] and phosphate[27], and appropriate fractions were lyophilized. The separation afforded O-polysaccharide (0.49 g) core oligosaccharide (0.43 g) and a fraction containing Kdo and phosphate (0.30 g).

ACKNOWLEDGMENTS

We thank Dr. D.E. Bradley, Memorial University of Newfoundland, St. John's, NF for the bacterial cultures, Mr. F.P. Cooper for the GLC–MS and FABMS analyses, Mr. D.W. Griffith for the large-scale production of bacterial cells, and Ms. L.L. MacLean for laboratory assistance.

REFERENCES

1 R.J. Rothbaum, A.J. McAdams, R. Giannella, and J.C. Partin, *Gastroenterology*, 83 (1982) 441–454.
2 M.R.F. Toleda, M.C.B. Alvariza, J. Murahovschi, S.R.T.S. Ramos, and L.R. Trabulsi, *Infect. Immun.*, 39 (1983) 586–589.

3 R.J. Rothbaum, J.C. Partin, K. Saalfield, and A.J. McAdams, *Ultrastruct. Pathol.*, 4 (1983) 291–304.
4 S. Tzipori, R. Gibson, and J. Montanaro, *Infect. Immun.*, 57 (1989) 1142–1150.
5 J.J. Mathewson and A. Cravioto, *J. Infect. Dis.*, 159 (1989) 1057–1060.
6 D.E. Bradley, A.N. Anderson, and M.B. Perry, *FEBS Microbiol. Lett.*, 80 (1991) 13–18.
7 O. Westphal, O. Luderitz, and F. Bister, *Z. Naturforsch., Teil B*, (1952) 148–155.
8 K.G. Johnson and M.B. Perry, *Can. J. Microbiol.*, 22 (1976) 29–34.
9 G.J. Gerwig, J.P. Kamerling, and J.F. Vliegenthart, *Carbohydr. Res.*, 77 (1979) 1–7.
10 K. Leontein, B. Lindberg, and J. Lönngren, *Carbohydr. Res.*, 62 (1978) 359–362.
11 K. Bock and C. Pedersen, *J. Chem. Soc., Perkin Trans. 2*, (1974) 293–297.
12 J.K.N. Jones and M.B. Perry, in K.W. Bentley (Ed.), *Technique of Organic Chemistry*, Vol. XI, Part II, Interscience Publishers, 1963, pp. 707–750.
13 B.B. Dimitriev, L.V. Backinowsky, V.L. Lvov, N.K. Kochetkov, and I.L. Hefman, *Eur. J. Biochem.*, 50 (1975) 539–547.
14 C. Erbing, K. Granath, L. Kenne and B. Lindberg, *Carbohydr. Res.*, 47 (1976) c5-c7.
15 I.J. Goldstein, G.W. Hay, B.A. Lewis, and F. Smith, *Methods Carbohydr. Chem.*, 5 (1970) 361–370.
16 G.A. Pearson, *J. Magn. Reson.*, 64 (1985) 487–500.
17 A. Bax and G.A. Morris, *J. Magn. Reson.*, 42 (1981) 501–505.
18 C. Altona and C.A.G. Haasnoot, *Org. Magn. Reson.*, 13 (1980) 417–429.
19 H. Bauman, P.-E. Jansson, and L. Kenne, *J. Chem. Soc., Perkin Trans. 1*, (1988) 209–217.
20 A. Bax, *J. Magn. Reson.*, 57 (1984) 314–318.
21 A. Dell, *Adv. Carbohydr. Chem. Biochem.*, 45 (1987) 19–71.
22 Yu.A. Knirel, N.A. Paramonov, E.V. Vinogradov, A.S. Shashkov, B.A. Dimitriev, N.K. Kochetkov, E.V. Kholodkova, and E.S. Stanislavsky, *Eur. J. Biochem.*, 167 (1987) 549–561.
23 S.W. Gunner, J.K.N. Jones, and M.B. Perry, *Can. J. Chem.*, 39 (1961) 1892–1895.
24 S. Hakomori, *J. Biochem. (Tokyo)*, 55 (1964) 205–208.
25 P.A. Sandford and H.E. Conrad, *Biochemistry*, 5 (1966) 1508–1516.
26 K. Kinns and J.K.M. Sanders, *J. Magn. Reson.*, 56 (1984) 518–520.
27 J.C. Richards and R.A. Leitch, *Carbohydr. Res.*, 86 (1989) 275–286.
28 M. Dubois, K.A. Gilles, J.K. Hamilton, P.A. Rebers, and F. Smith, *Anal. Chem.*, 28 (1956) 350–356.
29 R. Gatt and E.R. Berman, *Anal. Biochem.*, 15 (1965) 167–171.
30 D. Aminoff, *Biochem. J.*, 81 (1961) 384–392.
31 P.S. Chen, T.Y. Toribara, and H. Warren, *Anal. Chem.*, 28 (1956) 1756–1758.